

A NOVEL METALLURGICAL BONDING PROCESS AND MICROSTRUCTURAL ANALYSIS OF FERROUS ALLOY COMPOSITES

P.G. Huggett¹, R. Wuhler², B. Ben-Nissan³ and K. Moran⁴

¹ Materials Solutions Pty Ltd, 16 Ferntree Close, Thornlie WA 6108 Australia

² Microstructural Analysis Unit, University of Technology, Sydney, PO Box 123 Broadway Australia

³ Department of Chemistry, Materials and Forensic Sciences, University of Technology Sydney, Broadway Australia

⁴ Moran Scientific Pty Ltd, P.O. Box 651, Goulburn NSW 2580 Australia

ABSTRACT

A group of ferrous alloy composites have been produced using a novel vacuum casting process. The bonding and the interfacial analysis of these composites has been studied using various techniques including: optical microscopy, energy dispersive spectroscopy (EDS) microanalysis, X-ray mapping (XRM) and electron back scattered diffraction (EBSD). A number of phase changes and unique microstructural features have been observed. Some of these microstructural features are the result of the solidification process, whilst other changes have resulted from diffusion of elements across the composite interface. This study demonstrates the uniqueness of the vacuum casting process as an efficient bonding process and the importance of comparing data from a variety of analytical techniques to enable a thorough model of the solidification and diffusion processes to be properly developed.

1. INTRODUCTION

In general, ferrous alloy composites are produced using welding or brazing processes that require the two alloys being joined to have similar mechanical properties. Processes such as welding rely on the minimisation of weld dilution in combination with control of the energy input to provide an optimum joint strength and resultant mechanical properties and microstructure. Similarly, brazing has been employed to join dissimilar ferrous alloys, however the strength of the joint is limited due to the predominant mechanical jointing produced, and the need for close tolerances between the mating surfaces.

Vacuum brazing [1] has been used successfully to join white irons to mild steel through the use of a copper brazing alloy. The parts are heated to a temperature above the melting point of copper to allow the copper to wet both surfaces. The molten copper alloys with the iron to produce a columnar growth of copper/iron grains across the interface, with other elements diffusing across the interface.

Vacuum brazing requires close tolerances which can only normally be achieved through machining or grinding. The process is also reliant on the use of a brazing alloy such as copper (or sometimes nickel or other alloys). Due to the machining requirements and the need to use a brazing alloy, design and use of these ferrous alloy composites has been limited to blocks and plates which can be cost effectively cast in a foundry and machined to the required tolerances.

Additional complications arise between the two alloys being joined in vacuum brazing due to differences in thermal expansion between the two materials and the brazing material. The high stresses induced into the

parts can result in post heat treatment cracking of the parts, and substantial distortion.

White iron alloys have been successfully used in the mining industry to combat wear problems. The white iron has been used mainly in the form of castings, hard faced wear plates, and vacuum brazed composites of white iron and steel. The use of steel with the white iron as a composite imparts toughness to the wear parts, whilst also providing a means for more flexible attachment of the composites to equipment requiring wear protection.

The development of white iron compositions to optimise wear resistance has effectively reached a limit, and in order to further increase performance, and extend the use of white iron to new applications, composite techniques need to be used.

The CSIRO developed a process called Cast-Bonding [2], whereby white iron is cast directly onto steel substrates in a standard air atmosphere. The process requires the use of fluxes coating the steel substrate to limit oxidation. The steel substrate and mould are preheated to a moderate temperature of approximately 300 to 400°C, and the white iron cast directly onto the steel. The Cast-Bond process was successful in producing high quality bonds between the steel and the white iron, however minimal research was conducted at the time on the interface bonding mechanisms.

Recently a novel vacuum casting process has been developed to allow more complex composite shapes to be produced. The process permits the joining of steel to white iron when curved and complex shaped surfaces are involved. The process can also be used to repair worn components to near new original shapes. Unlike the vacuum brazing process, a bonding agent (eg.

copper) is not required, and surface preparation requirements are greatly simplified.

The vacuum casting process also permits the introduction of other compatible materials into the composite using one process. For example, tungsten carbide particles have been successfully introduced into the white iron region of the composite to further increase the wear resistance of the material [3].

2. EXPERIMENTAL PROCEDURES

Two types of samples were investigated. The first sample was a vacuum brazed white iron and mild steel bonded using a copper brazing agent produced by the vacuum casting process. The second sample was a white iron metallurgically bonded to a mild steel substrate with no brazing agent.

In vacuum casting of ferrous composites the materials consist of a high chromium white iron metallurgically bonded to a mild steel substrate. In order to enable the process to be suitable for common vacuum furnaces, a low melting point white iron was developed with a liquidus near 1200°C. The nominal composition of the white iron was Fe-12Cr-1.5Mn-1Ni-0.5Si-4C. Development of the low melting point white iron was based on the relationship between eutectic temperature and the carbon/chromium composition as shown in Figure 1 [4].

The vacuum casting process involves heating the substrate and the white iron in the form of ingots together in a vacuum heat treatment furnace, nominally to a temperature 50°C above the liquidus of the white iron. The temperature is held for a period of 60 minutes to allow the liquid white iron to react with the solid steel interface. The temperature is then reduced to solidify the white iron. At temperatures below the solidus of the white iron, solid state diffusion of the various alloying elements occurs.

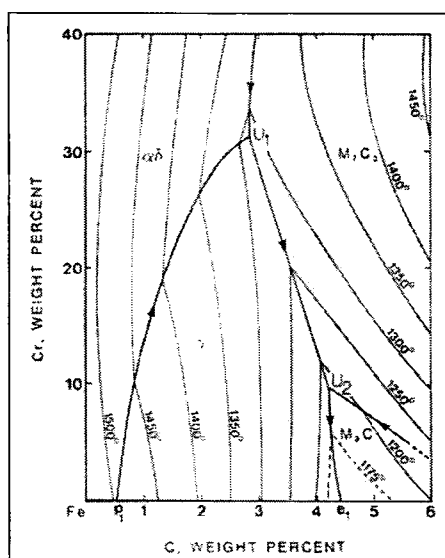


Figure 1: Liquidus Projection for the Fe-Cr-C System [4]

To contain the white iron in the liquid state during the melting phase of the process, the steel substrate can be used in the form of an integral mould. Alternatively the steel substrate can be placed within a reusable ceramic mould. The surface of the steel substrate is cleaned prior to the process to remove any existing oxide layers and contaminants. Parameters such as the pressure in the vacuum furnace, soak temperature, soak time, and cooling rate are all controlled to produce the final composite white iron bonded to the steel. Indeed, by varying these parameters, unique material properties can be obtained.

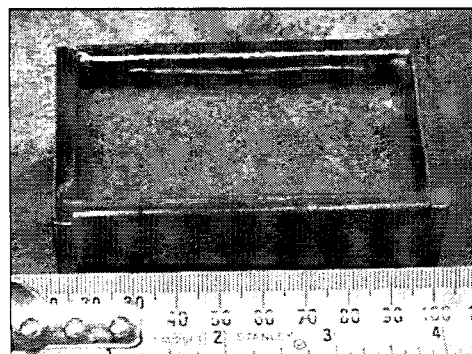


Figure 2: View of finished sample after removal from the vacuum tube furnace.

After the composite samples were produced (Figure 2), they were sectioned using standard metallographic techniques to enable the examination of the interfacial regions using optical microscopy, scanning electron microscopy, energy dispersive spectroscopy (EDS)[5], x-ray mapping (XRM) and electron back scattered diffraction (EBSD). Samples produced for EBSD analysis had the final mechanical damage from diamond polishing removed by chemical-mechanical polishing using colloidal silica.

X-ray maps were collected at 20kV accelerating voltages using a Moran Scientific energy dispersive x-ray analysis and mapping system attached to a Jeol 35CF SEM. A HKL Technology EBSD system attached to a LEO Supra 55VP FEG SEM was operated at 20kV accelerating voltage and 20mm working distance for EBSD mapping.

3. RESULTS

Typical x-ray maps for the vacuum brazed white iron and mild steel bonded using a copper brazing agent are shown in Figure 3.

These elemental x-ray maps shown in Figure 3 were used to generate scatter plots (Figure 4), where pixel frequency versus element concentration profiles were plotted against each other in two dimensions for selected elements within the sample. The clusters observed in these plots correspond to different phases within the composite interface. The contributing pixels to each cluster can be used to reconstruct the spatial distribution of its associated phase in a chemical image of the specimen (Figures 5 and 6).

The yellow highlighted regions of the images in Figures 5, 6 and 7 represent the compositional regions associated with the boxed areas of the scatter plots. Manipulation of the boxed areas on the scatter plots permits analysis of the composition for specific features observed in the microstructure.

Of particular interest to this study were the branches and links between clusters in each scatter plot and how these features correlate the chemical distribution of elements both in and around the bond region (Figure 7). The branching between the two nodes indicated a copper/iron phase, which could be an XRM artefact from the spatial resolution of the beam interaction volume. However, XRD and EBSD analysis revealed a copper/iron phase present. Furthermore, XRM at low accelerating voltages also revealed this phase present at the interface.

A typical optical micrograph of the second sample produced by the vacuum cast composite is shown in Figure 8. The micrograph demonstrates the excellent bonding between the two ferrous alloys, with no evidence of cracking at the interface. Furthermore, no brazing agent has been used to produce this sample.

Typical X-ray maps for the vacuum cast composite are shown in Figure 9. A secondary electron image and elemental maps of this interface region are shown for iron and chromium.

From the x-ray maps in Figure 9, scatter plots were generated which indicated three nodes were present with a possibility of a fourth node existing between two

nodes. However, better counting statistics were required for better accuracy.

Attempts to quantify the changes in microstructure around the bond interface using XRM's for the steel phase were restricted due to the very low concentrations of carbon present. The carbon content in the steel varies between 0.20 wt% to approximately 0.80 wt% at the interface, and this variation occurs within a distance of approximately 100 microns from the interface. Even though there was clearly a visual difference in the microstructure from low carbon steel for the original parent steel to almost fully eutectoid steel at the interface, the resolution of the XRM plots was not sufficient with respect to carbon content to permit suitable quantification of the changes observed. EBSD was used as an alternative method to improve the quantification of the microstructural and compositional changes of the interface region.

EBSD patterns for different areas around the interface for the vacuum cast composite were obtained and the Kikuchi patterns analysed to determine the crystal structures of the various phases. The EBSD maps produced were used to enable some quantification of the amount of phases present in various regions of the interface.

A higher magnification EBSD map of the eutectic carbides present in the white iron phase of the vacuum cast composite is shown in Figure 10.

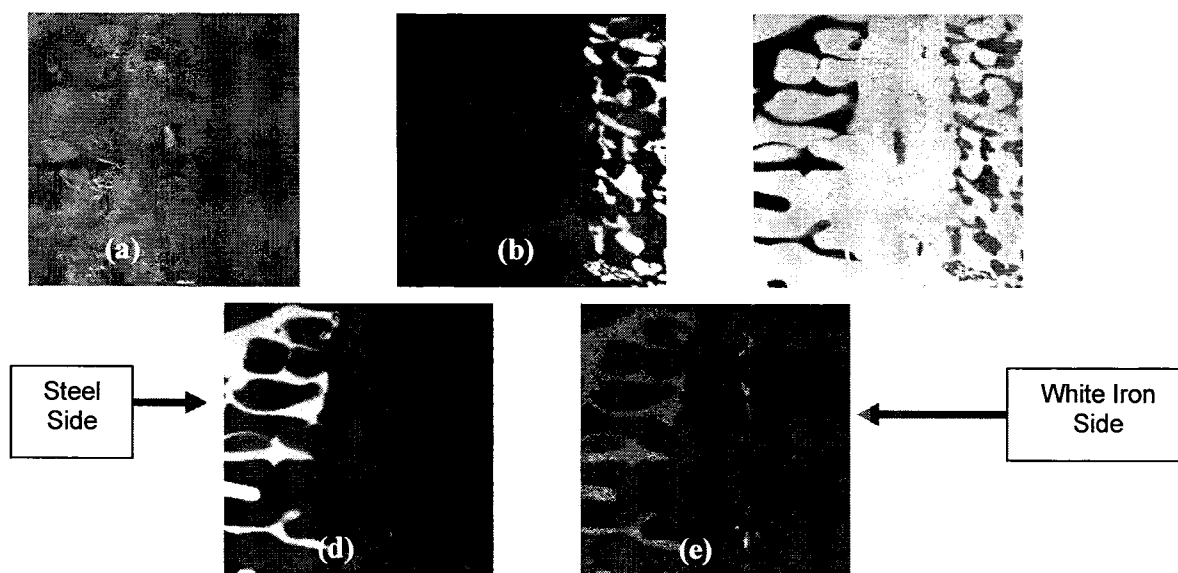


Figure 3: a) SEI Image, b) Cr map, c) Fe map, d) Cu map and e) Si map of the copper brazed white iron and steel interface (WOF = 160 μ m).

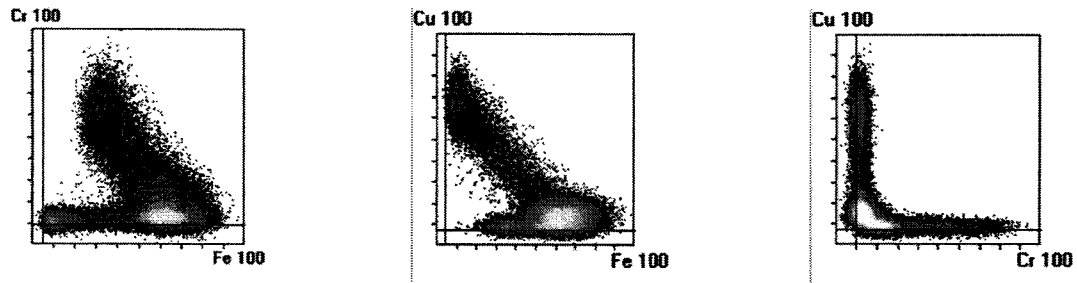


Figure 4: Scatter plots for vacuum brazed composite.

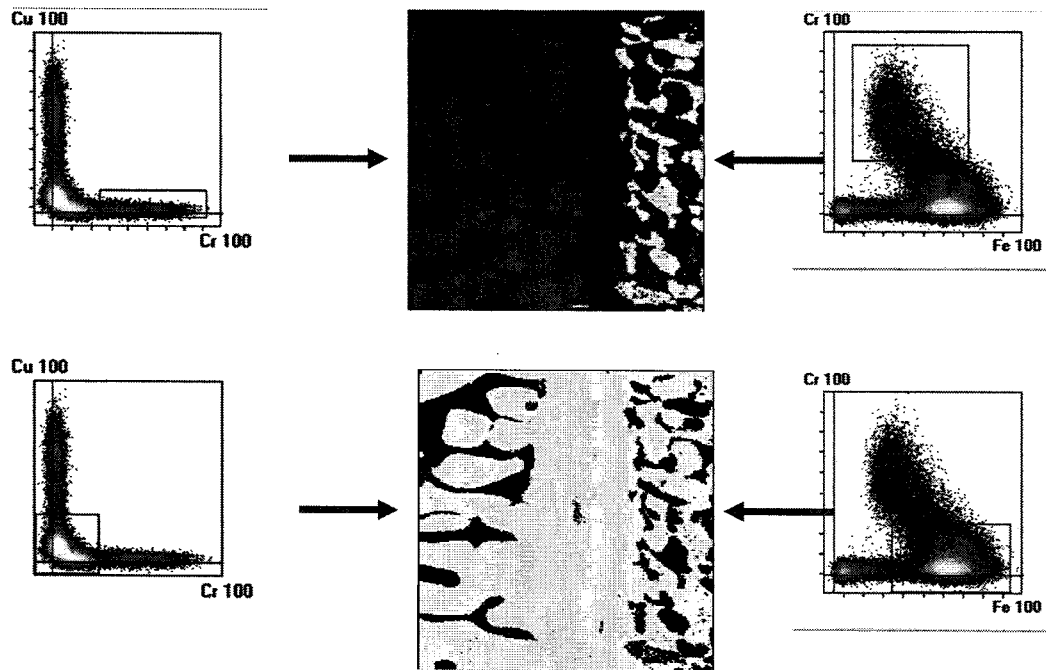


Figure 5: Scatter plots used to form chemical image for vacuum brazed composite ($WOF = 160\mu m$).

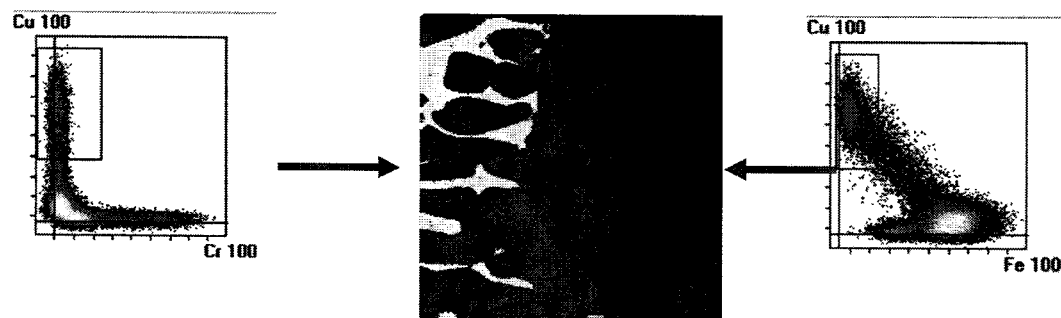


Figure 6: Scatter plots for copper/iron columnar grains in vacuum brazed composite.

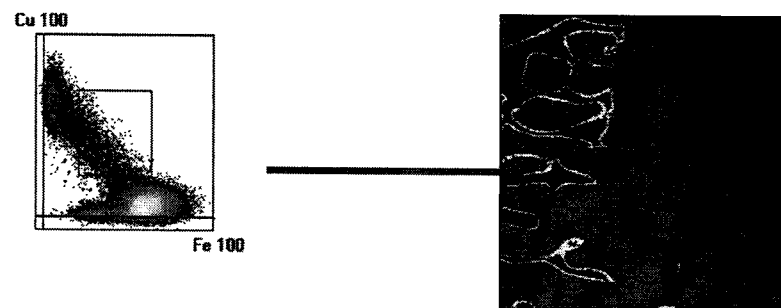


Figure 7: Scatter plots for grain boundaries between copper/iron columnar grains in vacuum brazed composite.

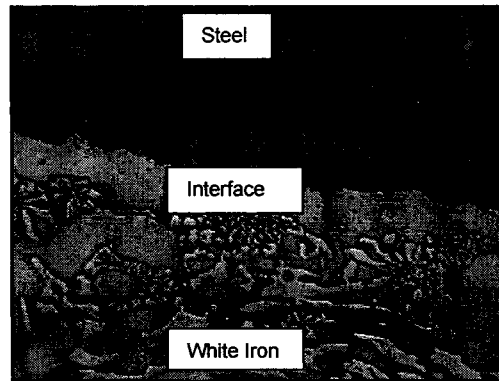


Figure 8: Typical optical micrograph of interface region between white iron and steel. (Etchant-acid ferric chloride).

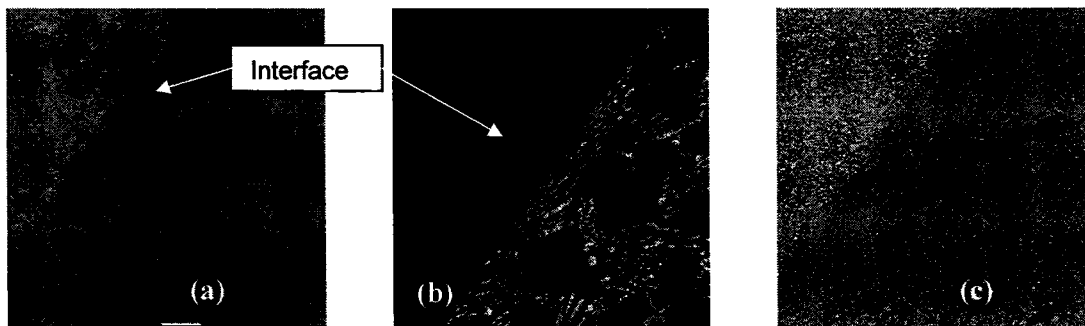


Figure 9: a) SEI Image, b) Chromium map and c) Iron map of the white iron and steel interface (WOF = 800 μm).

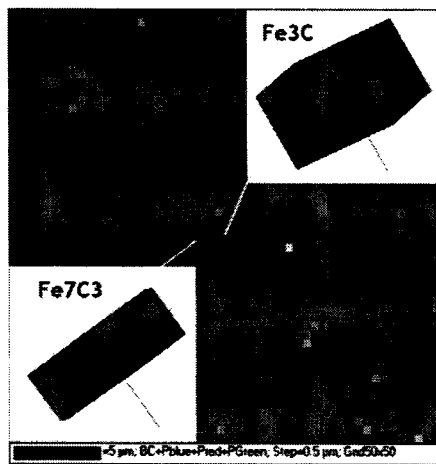


Figure 10: EBSD map showing M_7C_3 carbides surrounded by M_3C carbides in a ferrite iron phase

4. DISCUSSION

The results from the XRM analysis and scatter plots highlighted the diffusion of the alloying elements across the interface. The clusters observed in these plots correspond to different phases within the bond interface. The contributing pixels to each cluster can be used to reconstruct the spatial distribution of its associated phase in a chemical image of the specimen. Of particular interest to this study were the branches and links between clusters in each scatter plot and how these features correlate to the chemical distribution of

elements both in and around the bond region. Preliminary analysis indicated these links and branches in the scatter plot correspond to solid solutions between chemical phases and diffusion gradients.

The interface developed for the sample with no brazing agent from the vacuum casting process exhibits four distinct zones. Zone 1 is the parent steel substrate, which in this example was 0.2% C steel. This region consists of 75% ferrite and 25% pearlite. Zone 2 is the transformed parent steel adjacent to the liquid/solid interface with the white iron. This zone exhibits a transformed microstructure of hypereutectoid steel, predominantly of pearlite, with some Fe_3C carbides precipitating along a perpendicular alignment to the primary steel/white iron interface.

Zone 3 is the white iron region adjacent to the liquid/solid interface, and is remarkable for the absence of eutectic carbides of the M_7C_3 type normally associated with high chromium white irons. Significantly, M_3C carbides have formed as a continuation of the Fe_3C carbides in Zone 2.

Zone 4 represents the remainder of the white iron region, exhibiting eutectic M_7C_3 carbides with a ferrous matrix. The four zones are highlighted in Figure 11.

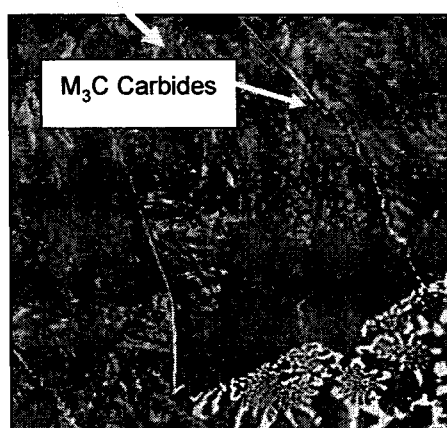
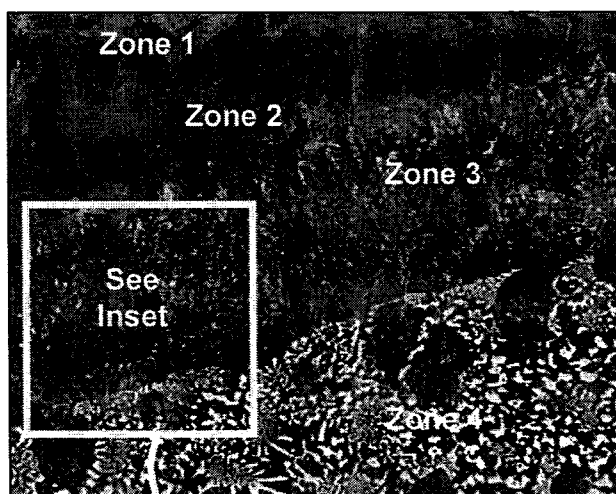


Figure 11: Material zones in white iron/steel composite produced from vacuum casting (Optical micrograph, etchant: acid ferric chloride)

The EBSD results for the carbides in Zone 4 revealed M_7C_3 carbides surrounded by M_3C carbides with similar orientation in a ferrite iron phase. These EBSD results provide a greater insight into the solidification sequence at the bond interface, with far greater resolution compared to other techniques such as EDS and XRD analysis.

The vacuum casting process was used to manufacture a range of composite wear parts for use in mining applications. One particular trial incorporated a white iron/steel composite ground engaging tool (GET) located on a suction-cutter dredge at a mineral sands mine in Capel, Western Australia.

The composite wear tooth operated for a period of eight weeks compared to the original steel wear tooth operating life of two weeks. The increase in wear life can be attributed to the white iron coating on the wear tooth. The worn components showed no presence of brittle fracture or debonding of the white iron.

5. CONCLUSION

A novel method of manufacturing ferrous composites has been outlined that provides an exceptional bond. The manufacturing method permits the bonding of white iron onto steel substrates without the need for pre-machining, and provides greater flexibility in sample geometries. SEM, EDS, XRM and EBSD analysis has shown the vacuum casting process promotes a full metallurgical bond, and has enabled the elemental distributions to be studied to provide an improved understanding of the bonding mechanism. Further work particularly with the interpretation of the scatter plots as well as the EBSD results will provide an enhanced understanding of the chemical processes involved in the bonding of dissimilar materials. Field trials conducted on composite wear parts manufactured using the vacuum casting process demonstrated a significant improvement in operating life.

REFERENCES

1. T. Yoshida and H. Ohmura: *Welding Journal*, 1980, Vol. 59, No. 10, pp278-282
2. T. Heijkoop and I.R. Sare: *Cast Metals*, 1989, Vol. 2, No 3, pp160-168
3. R. Wuhler, K. Moran, P. Huggett, M.R. Phillips, and B. Ben-Nissan: *Proc. of Microscopy and Microanalysis 2004*, Savannah USA, Cambridge University Press, 2004
4. W.R. Thorpe and B. Chico: *Metallurgical Transactions*, 1985, Vol. 16A, pp1541-1549
5. J.I. Goldstein, M.R. Notis and A.D. Romig: *Diffusion in Solids: Recent Developments*, Metallurgical Society, 1984, pp167-193